Performance Evaluation of RSSI-based Positioning System with Low-cost LoRa Devices

Christian Sanchez
chrispsan@hotmail.com
Cuenca, Ecuador

Braulio Arpi
braulio.arpi.pc@gmail.com
Cuenca, Ecuador

Andres Vazquez-Rodas
andres.vazquezr@ucuenca.edu.ec
Universidad de Cuenca
Cuenca, Ecuador

Fabian Astudillo-Salinas
fabian.astudillos@ucuenca.edu.ec
Universidad de Cuenca
Cuenca, Ecuador

Luis I. Minchala
ismael.minchala@ucuenca.edu.ec
Universidad de Cuenca
Cuenca, Ecuador

ABSTRACT

Along the last years, we have witnessed the growing demand for services, applications, and systems that depend on the specific location of both people and a variety of things and gadgets. Currently, the Global Positioning System (GPS) offers good accuracy on-location services around the world. Nevertheless, it does not work efficiently on applications that require several small, cheap, and low power devices. Under such conditions, researchers prefer to work with low-cost wireless alternatives such as WiFi, Zigbee, LoRa, Sigfox, among others. The purpose of this work is twofold. Firstly we evaluate the time-measurement and radio frequency capabilities of Pycom LoRa hardware implementation, in order to develop a low-cost and GPS-independent positioning system. Then, with these results, we propose and evaluate a positioning system with LoRa technology and based on the received signal strength indicator. Extensive field test measurements in outdoor rural environments show that we can obtain position estimation errors lesser than around 7% of the maximum distance between anchor nodes.

CCS CONCEPTS

• **Networks → Network performance analysis**; *Network experimentation*; Network simulations.

KEYWORDS

LoRa; Positioning System (PS); RSSI; TDoA; ToA

ACM Reference Format:

Christian Sanchez, Braulio Arpi, Andres Vazquez-Rodas, Fabian Astudillo-Salinas, and Luis I. Minchala. 2019. Performance Evaluation of RSSI-based Positioning System with Low-cost LoRa Devices. In *16th ACM Symposium on Performance Evaluation of Wireless Ad Hoc, Sensor, & Ubiquitous Networks (PE-WASUN '19), November 25–29, 2019, Miami Beach, FL, USA.* ACM, New York, NY, USA, 8 pages. https://doi.org/10.1145/3345860.3361512

Permission to make digital or hard copies of all or part of this work for personal or classroom use is granted without fee provided that copies are not made or distributed for profit or commercial advantage and that copies bear this notice and the full citation on the first page. Copyrights for components of this work owned by others than the author(s) must be honored. Abstracting with credit is permitted. To copy otherwise, or republish, to post on servers or to redistribute to lists, requires prior specific permission and/or a fee. Request permissions from permissions@acm.org.

PE-WASUN '19, November 25–29, 2019, Miami Beach, FL, USA

© 2019 Copyright held by the owner/author(s). Publication rights licensed to ACM.

ACM ISBN 978-1-4503-6908-4/19/11…$15.00
https://doi.org/10.1145/3345860.3361512

1 INTRODUCTION

Today, it is very important to localize people or objects for almost every life activity. Just to quote an example, in the commercial field, the location knowledge of the products of a company is fundamental to reduce the search and operation times, and as a result productivity is improved [1].

The most utilized location method around the world is the global positioning system (GPS). However, one the of main disadvantage of GPS is its high power consumption and cost, which prohibits its large-scale deployment [2]. Nowadays, new low cost and low power consumption wireless technologies are emerging, which allow the deployment of densely distributed networks for a wide range of applications. Among them, stands out environmental monitoring, humans, animals, or vehicles monitoring [3, 4], athletes tracking [5], etc. In such applications, it is very important to optimize the power consumption and the total network deployment costs. In general, data rate requirements of such applications are less demanding. In this context, it is important to consider solutions based on the emerging low-power wide-area networks (LPWANs) which can efficiently operate over large areas and with battery-powered devices [6, 7].

At present, the more relevant LPWANs are: LoRa [8], Sigfox [9], and NarrowBand IoT (NB-IoT) [10]. Many research works have shown the advantages of the new physical layer LoRa technolgy and its upper layer LoRaWAN complement regarding scalability, coverage, and energy efficiency [11, 12]. From [13] it is apparent that LoRa technology has greater potential to develop a positioning system alternative to GPS in comparison with the other LPWANs. Of course, other wireless technologies such as WiFi or Zigbee are useful for the development of low cost positioning systems.

On the other hand, the most common positioning algorithms are time of arrival (ToA), time difference of arrival (TDoA), angle of arrival (AoA), and received signal strength indicator (RSSI). Each of these algorithms requires that wireless devices present different features and hardware capabilities. Additionally, these last algorithms are complemented with the localization algorithms such as multilateration, triangulation, and trilateration.

On this basis, this work presents a deeper evaluation of a hardware implementation of LoRa technology, specifically the LoPy and FiPy devices of Pycom manufacturer. The evaluation focuses on the study of the time measurement capabilities of the devices in order to implement a time-based positioning system for real environments.

We also evaluate the quality of the radio frequency components in order to implement a positioning system based on RSSI variable. Finally, with these results, we implement and evaluate a low-cost RSSI-based positioning system. We evaluate the performance of the system through extensive field test measurements on outdoor rural environments of Cuenca-Ecuador.

2 BACKGROUND

Positioning systems can be broadly classified in one of the following categories: global positioning systems, which allows the localization of targets around the globe, or local positioning systems, which allow the localization of targets in a local environment of established size [14]. This work focuses on local positioning systems and this section presents a brief background on position estimation algorithms.

The time of arrival (ToA) position estimation algorithm gets the distance between the target node (TN) and each anchor node (AN) through the travel time measurements of the respective reference signals. Then, with a minimum of three anchor nodes with known positions and strict time synchronization, it is possible to localize the target node using a trilateration approach (Figure 1). Meanwhile, the time difference of arrival (TDoA) estimation relaxes the synchronization requirements between the target node and the anchors, just anchor nodes must be synchronized. And in general, it overcomes the drawbacks of ToA.

In the angle of arrival (AoA) estimation, the anchor nodes estimate the target location based on the angle of the respective arriving signal. In a coplanar scenario, AoA requires just two anchor nodes, but they must equipped with smart antenna arrays.

On the other hand, in the estimation based on the received signal strength indicator (RSSI), the anchor nodes estimate the target location mapping the RSSI with the distance traveled by the signal. It requires a path loss model to estimate such distance. Then, in the same way that ToA with a minimum of three anchor nodes the target node position is estimated by trilateration (Figure 1) [14].

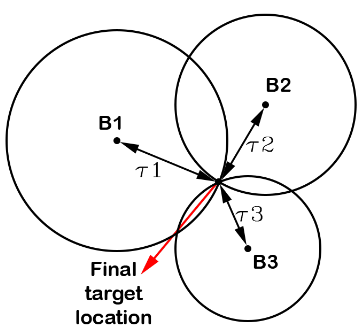

Figure 1: ToA and RSSI position estimation approach.

We can get the RSSI logarithmic model equation through a minimum squares fitting of the RSSI field measurements (Eq.1). Here, c and b, are constants.

$$y = c \times \ln x + b \tag{1}$$

For ToA and RSSI, in a 3D scenario, the target node location is determined by the intersection of all spheres, whose centers are the coordinates of the anchor nodes and the radii are the distances between the anchor nodes and the target node (Eq. 2).

$$(x - x_i)^2 + (y - y_i)^2 + (z - z_i)^2 = m_i^2, (i = 1, 2, ..., n) \tag{2}$$

Where (x_i, y_i, z_i) are the known coordinates of anchor nodes, m_i are the estimations of the distance between the anchors and the target node, and n is the number of anchor nodes. In this way, solving this equation, we get the target node coordinates (x, y, z). Then, the trilateration localization algorithm derives from this fundamental Eq. 2, which is the math basis for the ToA or RSSI based positioning systems. In the case of a 2D scenario with three anchor nodes, we get the system of second-order equations shown in Eq. 3.

$$\begin{cases} (x - x_1)^2 + (y - y_1)^2 = m_1^2 \\ (x - x_2)^2 + (y - y_2)^2 = m_2^2 \\ (x - x_3)^2 + (y - y_3)^2 = m_3^2 \end{cases} \tag{3}$$

In this work, we use an analytical model to solve this system of equations and to implement them in the proposed positioning system.

3 RELATED WORK

Several recent works focus on the implementation of low-cost and energy efficient positioning systems based on LoRa Technology. For example, authors in [15] propose an hybrid LoRa-GPS tracker for dementia patients. The main objective of this work is to improve the energy efficiency of the GPS system by integrating LoRa communications and using a GPS duty cycling strategy. In [16] authors propose a TDoA LoRa positioning system which uses a multilateration location algorithm. Although authors entitle their proposal as GPS-free geolocation, the end-nodes and the gateways incorporate GPS for synchronization purposes. This work presents an accuracy of around 100 m in a 2 km × 2 km urban area. The LoRa Alliance in [17] presents a compilation of technical capabilities of LoRaWAN-based geolocation. The work focuses on new generation of LoRaWAN gateways which incorporate TDoA positioning algorithm capabilities. Paper also include real deployment case studies, with this specialized high cost gateways, such as in Barcelona port, the urban environment of Issy-les-Moulineaux, Bolougne next to Paris, and among others.

This work focuses on a deeper evaluation of the capabilities of low cost Pycom LoRa hardware implementation, in order to develop a totally GPS-independent positioning system. We also include the performance evaluation of a RSSI-based positioning system through field test on rural environments.

4 PERFORMANCE EVALUATION OF LORA DEVICE CAPABILITIES

The purpose of this section is to evaluate the performance of LoPy and FiPy LoRa devices regarding their time measurement capabilities, RSSI sensitivity, and dynamic range.

4.1 LoPy and FiPy devices description

LoPy and FiPy are low-cost development boards produced by Pycom manufacturer, which include LoRa technology [18]. Table 1 summarizes the more relevant technical features of these boards. Besides, these devices have incorporated a 150 kHz real-time clock

(RTC) and a RSSI sensitivity sensor. In this section, we evaluate the real performance of these two last characteristics through field measurements. The goal is to determine if they are suitable for either time or RSSI based positioning system.

Table 1: Technical features of LoPy and FiPy devices [19, 20].

Feature	LoPy 1.0 and FiPy
RTC (kHz)	150
ISM bands (MHz)	868, and 915
Semtech [21] chip	*SX*1272
Range (MHz)	860 − 1020
SF	6 − 12
BW (kHz)	125 − 500
Data Rate (kbps)	0.24 − 37.5
RSSI sensitivity (dBm)	−117 to −137

It is important to note that the RSSI sensitivity of the LoRa devices vary in function of the operation bandwidth (BW) and spreading factor (SF).

In this context, Table 2 presents the RSSI sensitivity of LoPy and FiPy devices under different BW and SF configurations.

Table 2: RSSI Sensitivity of LoPy and FiPy devices [19, 20].

BW (kHz) and SF	LoPy 1.0 (dBm)	FiPy (dBm)
125 and 6	−121	−122
250 and 12	−134	−135
500 and 12	−129	−131

4.2 Evaluation of LoPy and FiPy time measurement capabilities

Time-based positioning algorithms such as ToA or TDoA have strict requirements regarding the time measurement capabilities of the devices. For LoPy and FiPy boards we identify and evaluate three different ways to measure and estimate the round trip time (RTT): (1) through the built-in chronometer function, (2) using the internal RTC, and (3) through the CPU instruction or cycle time.

In order to evaluate and compare the real time measurement capabilities of LoPy and FiPy devices, we develop a set of field tests in which we establish a communication link between the target node and one anchor node. We measure the RTT for three different distances (15 m, 2.6 km, 10 km) between the target and anchor nodes. For each evaluation point, the target node sends a message, then the anchor replies with an echo. After that, the target measures and estimates the RTT using one of the previously mentioned evaluation methods. In order to present reliable results, the target node repeats the experiment around 200 times for each point and we report the average RTT with 95% confidence interval.

Figure 2 compares the resulting RTT estimation using the chronometer function, the internal RTC, and the CPU cycle method respectively. From this figure, we can conclude that, with these low-cost devices, no one of the RTT estimation methods present suitable results for a time-based positioning system development. We can observe an overlapping of confidence intervals of the measured RTT for all the cases with the chronometer function estimation. We can also see that the built-in chronometer function presents more variable results in comparison with the other two methods. Finally, for RTC and CPU cycle we can observe also an overlapping of the confidence intervals of the RTT between the measurements at 15 m and the measurements at 2.6 km, and a slight time difference for the 10 km distance.

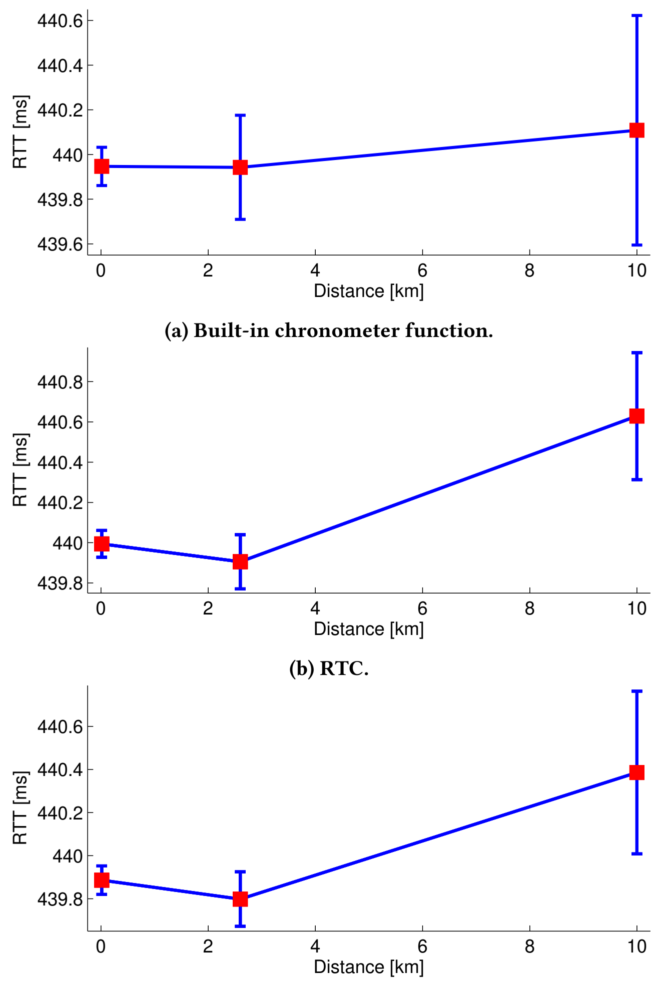

(a) Built-in chronometer function.

(b) RTC.

(c) Ticks, instruction time or CPU cycle.

Figure 2: Performance results of three different methods of RTT measurements, with BW= 500 kHz, SF = 12 and P_{TX} = 20 dBm.

4.3 Evaluation of RSSI sensitivity and dynamic range

LoPy and FiPy devices allow the configuration of their LoRa modulation RF features such as: transmission power (P_{TX}), bandwidth, and spreading factor. As expected, these different configuration possibilities have a direct impact on the device RSSI sensitivity, as reported by the manufacturer in Table 2. Accordingly, in this section we evaluate the real dynamic range and sensitivity of LoPy and FiPy devices through controlled field tests.

The controlled field test consists of establishing a communication link between a LoPy 1.0 transmitter and other LoPy 1.0 receiver. In order to control the attenuation of the transmission power, the LoPy transmitter is connected to a Hewlett Packard (HP) 8496B variable attenuator (Figure 3). This HP attenuator has a resolution of 1 dB, and its attenuation ranges from 1 to 121 dB.

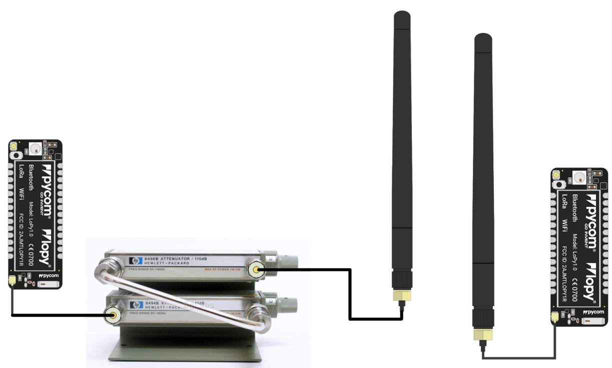

(a) T_X **device with variable attenuator.** **(b)** R_X **device.**

Figure 3: Dynamic range tests of RSSI sensitivity.

We evaluate the LoPy RSSI behavior under two different configurations of P_{TX}, BW, and SF. The first set of tests was done with $BW = 500$ kHz, and $SF = 12$. In turn, the second set used a $BW = 125$ kHz, and a $SF = 7$. In both cases we evaluate the system configured with the minimum and the maximum allowed transmission power corresponding to 5 dBm and 20 dBm respectively. Furthermore, we establish and evaluate three different separation distances between the transmitter and the receiver ($d = 10$ m, $d = 30$ m, and $d = 50$ m). In turn, for each separation distance, we vary the attenuation from 0 dB to 50 dB with 5 dB steps.

Figure 4 shows the resulting RSSI value evolution measured by the receiver node, for each described test. From Figure 4b, in first place, we can observe that when the system is configured with $BW = 125$ kHz, and a $SF = 7$ the behavior of the RSSI is more unpredictable and so the dynamic range in this case is not clear. Thus, this configuration does not allow to have a good characterization of the communication link between the transmitter and the receiver. Then, this configuration is not suitable for a RSSI-based positioning system. On the other hand, for the system configured with $BW = 500$ kHz, and $SF = 12$, on Figure 4a, we observe a stable behavior of the RSSI variable for all the cases until an attenuation of around 30 dB, which corresponds to a RSSI value greater than around -110 dBm. This implies that the dynamic range of LoPy devices is suitable for a RSSI-based positioning system development for values of RSSI greater than -110 dBm and when the LoRa modulation is configured with $BW = 500$ kHz, $SF = 12$ and $P_{TX} = 5$ dBm. Another observation from the field tests is the fact that different LoPy and FiPy devices, in spite of using the same chip Semtech

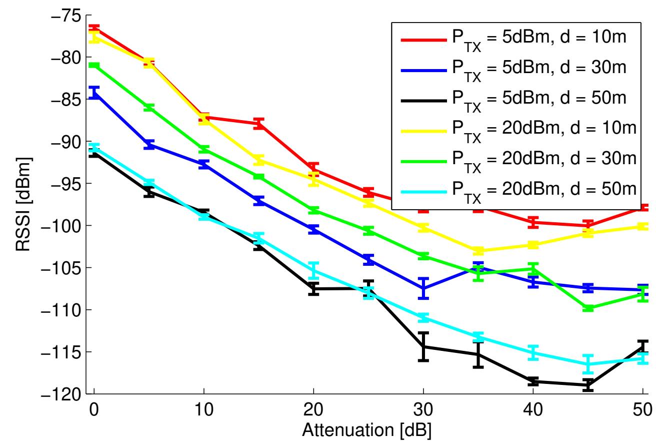

(a) Test 1 with $BW = 500$ **kHz and** $SF = 12$.

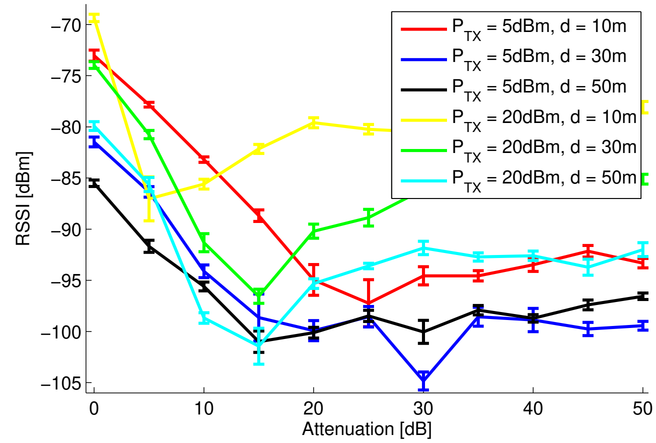

(b) Test 2 with $BW = 125$ **kHz and** $SF = 7$.

Figure 4: Field controlled tests of links between a LoPy 1.0 as T_X **with variable attenuator and other LoPy 1.0 as** R_X**.**

SX1272 [21], exhibits different behaviors regarding RSSI sensitivity and dynamic range. Additionally we expect a greater impact of the selected transmission power over the resulting RSSI values. These two facts motivated us to make a deeper analysis of the real transmission power of the LoPy and FiPy devices and its variability.

4.4 Evaluation of the transmission power

In order to make a deeper and reliable evaluation of the LoPy and FiPy devices transmission power, we use as a receiver a National Instruments PXI system. For this test set, the LoPy or FiPy transmitter is connected to the attenuator configured with an attenuation value of 30 dB to guarantee that the power keeps in the range accepted by the PXI receiver module. Each device is evaluated for its minimum ($P_{TX} = 5$ dBm) and its maximum ($P_{TX} = 20$ dBm) transmission power.

The first test was done with a FiPy device configured with the following LoRa modulation parameters: $P_{TX} = 5$ dBm and $BW = 500$ kHz. Since we use an attenuation of 30 dB we expect that the received power in the PXI system to be around −25 dBm. However, as it can be observed in the Figure 5a, the real received power is −29.74 dBm. Thus for this FiPy device we obtain a power error of −4.74 dBm. We also observe a real transmission bandwidth of $BW = 608.97$ kHz. Then, it is around of 108.97 kHz out of band emission.

In the second case, the FiPy device was configured with $P_{TX} = 20$ dBm and $BW = 500$ kHz. Figure 5b presents the resulting power and BW reported by the PXI for this configuration. We observe a received power of -23.75 dBm, so an error of -13.75 dBm is obtained. Thus, when the device is configured with the maximum transmission power, the error of the power amplifier is significantly increased. Regarding the BW error it remains the same as the previous case (108.97 kHz).

In turn, for the LoPy device configured with $P_{TX} = 5$ dBm and $BW = 500$ kHz, the resulting power error is around −0.94 dBm as it is depicted in the Figure 5c. The measured BW is 528.84 kHz so the obtained error is 28.84 kHz. Finally, when the LoPy device is configured with the maximum transmission power $P_{TX} = 20$ dBm and BW= 500 kHz, the power error is −1.97 dBm as it can be see in the Figure 5d. For this last case the measured transmission BW is 520.83 kHz and therefore we obtain a 20.83 kHz out of band emission.

Therefore, we can conclude that the radio frequency components of LoPy 1.0 devices and its RF accessories are of better quality than the FiPy devices. Also, in order to have a better behavior of the positioning system, the preferred configuration of LoRa modulation parameters for this kind of devices is $BW = 500$ kHz, $SF = 12$ and $P_{TX} = 5$ dBm.

5 RSSI-BASED POSITIONING SYSTEM

Based on the LoPy and FiPy devices detailed evaluation presented in the Section 4, in this section we start defining the proposed RSSI-based positioning system architecture and then we present the performance evaluation of the system.

5.1 System Architecture

For the proposed positioning system, we choose an architecture centralized on the target node. We do not use any specialized gateway, with dedicated localization features, with the purpose of keep at the minimum the system costs. Then, in such architecture, the target node establishes a communication link with each anchor node at a time, following a round-robin type procedure (Figure 6). The aim of each link is to measure and store the value of the RSSI variable resulting of the communication between the target node and the respective anchor node. After that, using the RSSI-based positioning and the trilateration localization algorithm, we estimate the location of the target node.

As we observe in the Figure 6, there are three main components in the positioning system, the target node, the anchor nodes, and the main processor. We also identify two communication links: (1) The link between the target node and each of the anchor nodes using a LoRa interface to send request messages and to obtain relevant values such as RSSI and SNR. (2) The communication link between the target node and the processor through a WiFi interface. We use the FTP protocol to get the variable registers from the internal memory of the target node to the processor system.

The LoRa communication link between the target node and each anchor node follows the messages sequence shown in Figure 7. The target node sends a request to one anchor node, identified with 1 Byte of unique identity field included in the payload of the LoRa frame. Then, the anchor node with such identity sends a reply message. For the positioning system, the reply message corresponds to the return link and we also measure the RSSI value of this link.

5.2 Performance Evaluation

The positioning system uses two relevant RSSI measurements on each link between the target node and the anchor nodes. Specifically, the RSSI value of the forward link measured by the anchor node, and the RSSI of the return link measured by the target node. In this way, we analyze the performance of the system under three different approaches. (1) The location of the target using only the RSSI of the forward link. (2) The location of the target using only the RSSI of the backward link. (3) The location of the target using the average RSSI value of the forward and return links.

The evaluation is based on field test measurements, carried out in the rural area of Pachamama in Cuenca-Ecuador ($2°49'58.72''S$; $78°55'43.75''O$). This is a flat land of around 500 m × 500 m and all the communication links are with line of sight (LoS). Among others, we consider and report here the evaluation for two square area scenarios. One of 90 m × 90 m, and the other of 150 m × 150 m. In both cases we consider a symmetric distribution of four anchor nodes, one on each corner of the square.

Firstly, it is necessary to characterize each communication link between the target node and each of the anchor nodes. The aim is to obtain the path loss model of each link through a least squares adjustment of the RSSI values. For illustration purposes, Figure 8 shows such resulting characterization for the return link of the 90 m × 90 m scenario. We follow a similar procedure for the forward link, the round trip link, and for the 150 m × 150 m scenario.

5.2.1 Results analysis. One of the field measurement study was done in the 90 m × 90 m previously described scenario. We use four anchor nodes with identifiers A, B, C y D and fixed positions at the corners $(0, 0)$, $(0, 90)$, $(90, 90)$, $(90, 0)$ respectively. Table 3 summarizes the real position of the target node for five different test points. As previously said, we evaluate the performance of the positioning system for three different approaches: using only the RSSI value of the forward link, denoted by (e_1), the RSSI of the return link (e_2), and the average RSSI of the forward and return links (e_3). Since we use four anchor nodes, therefore, there are one useful estimation through the trilateration localization algorithm. On the other hand, it is important to note that if we use the RSSI information of just three of the anchor nodes for the trilateration algorithm, by combinatorics, there are $C_4^3 = 4$ possible useful position estimations. Then, we have a total of five valid possible position estimation for this reported test. We compute and select the centroid point of the whole set of estimations as the better approximation of the target position. In this context, we evaluate the accuracy of the system by means of the position estimation error, which in turn, is the distance between the real position and the estimated position of the target.

Table 4 summarizes the position estimation error of the system for each of the above described approaches. From these results,

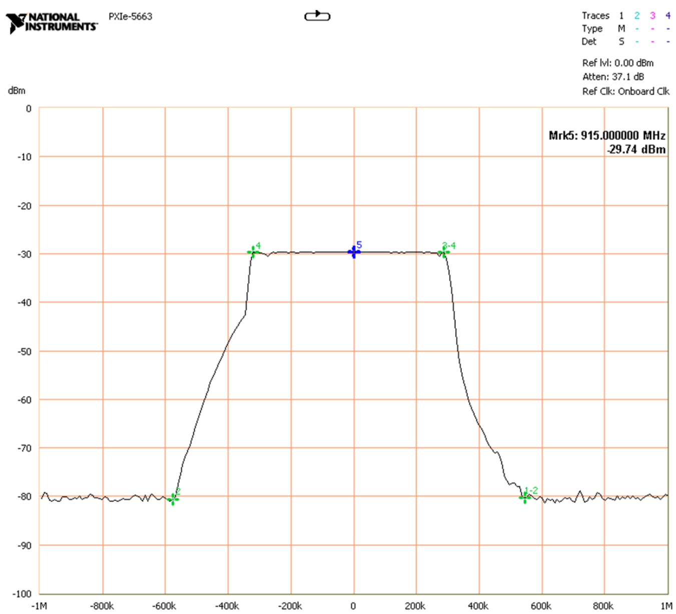

(a) FiPy with $P_{TX} = 5\,\text{dBm}$

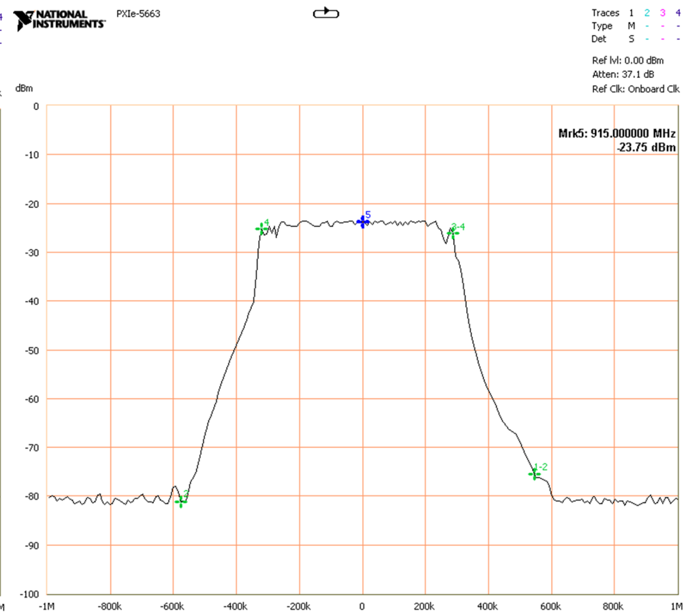

(b) FiPy with $P_{TX} = 20\,\text{dBm}$

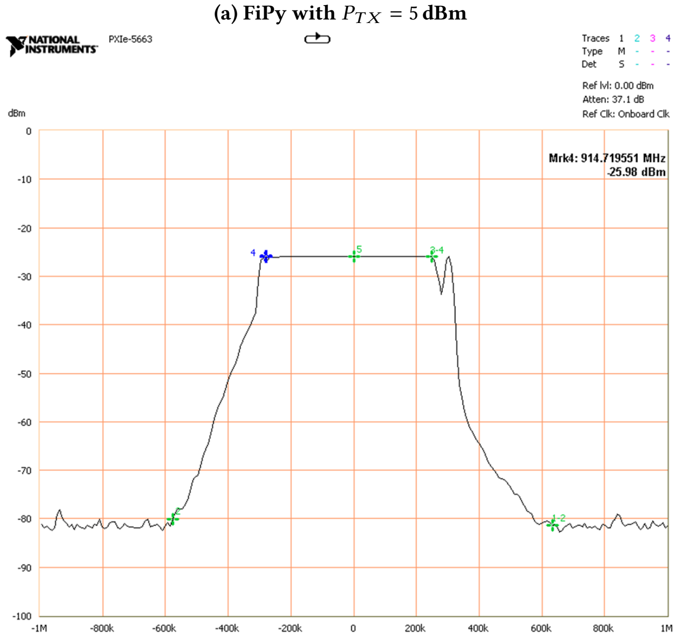

(c) LoPy 1.0 with $P_{TX} = 5\,\text{dBm}$

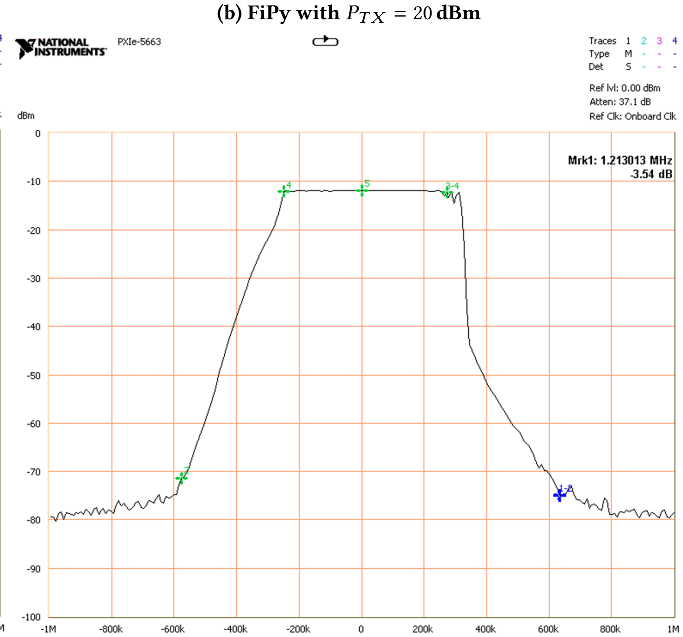

(d) LoPy 1.0 with $P_{TX} = 20\,\text{dBm}$

Figure 5: Power transmission evaluation of LoPy and FiPy devices with BW= 500 kHz, SF= 12 and 30 dB of attenuation

we can conclude that the use of the RSSI value of the return link presents a better approximation than the other two methods. In fact, the percentage of the average estimation error of this method is around the half of the error resulting with the other two methods.

Additionally, we evaluate the positioning system in a bigger area of 150 m × 150 m. We also use four anchor nodes located at the corners of this square area. Table 5 shows the real position of the target node for the five different test points. While Table 6 summarizes the

Table 3: Real position of the test points for the 90 m×90 m scenario.

Point	P_7	P_8	P_9	P_{10}	P_{11}
x (m)	35.35	56.56	54.64	45	33.43
y (m)	35.35	56.56	35.35	45	56.56

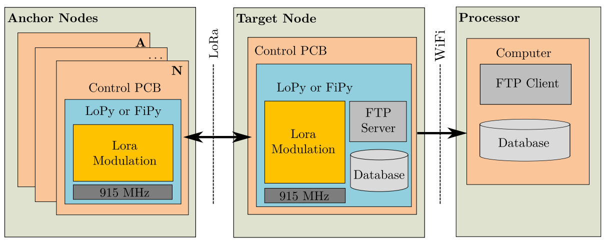

Figure 6: General Architecture.

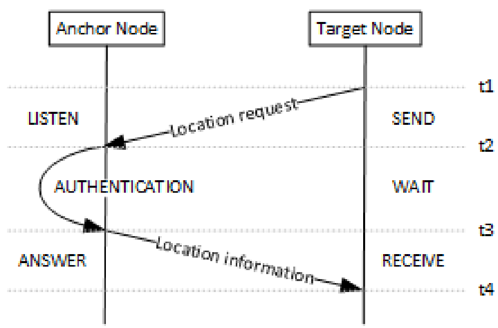

Figure 7: Sequence diagram of the link between the target node and one anchor node.

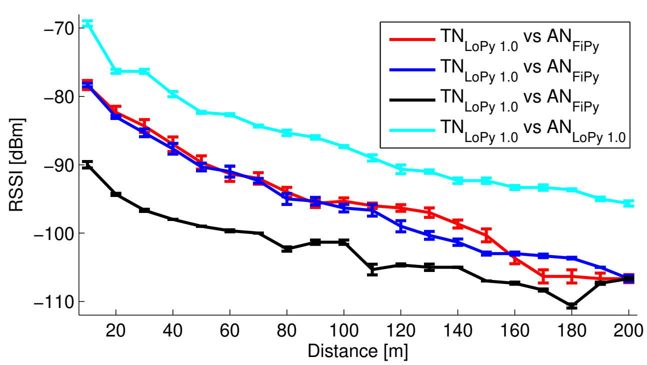

Figure 8: The characteristic curve of the return link for the 90 m×90 m scenario with BW = 500 kHz, SF = 12 y P_{TX} = 5 dBm.

Table 4: Position estimation error for the first scenario.

e_{link}	P_7	P_8	P_9	P_{10}	P_{11}	$\bar{e}$ (m)	(%)
e_1 (m)	7.44	11.05	22.30	26.07	23.22	18.01	14.15
e_2 (m)	8.19	8.54	12.60	1.36	12.06	8.55	6.72
e_3 (m)	7.49	10.84	21.61	18.27	19.89	15.62	12.27

position estimation error for this case. According to these results, and for this second scenario, we obtain a better accuracy using the RSSI information of the forward link. It is important to note that in no case the use of the average RSSI value of the forward and the return link present a better approximation. This is due to the great variability of each link and as a whole. It is also required to make a previous analysis of the behavior of the system for each operation scenario. This in order to define the more suitable approach which will result in the lesser localization error than the other approaches.

Table 5: Real position of the test points for the 150 m×150 m scenario.

Point	P_{17}	P_{18}	P_{19}	P_{20}	P_{21}
x (m)	63.63	84.85	86.36	75	65.14
y (m)	63.63	84.85	63.63	75	84.85

Table 6: Position estimation error for the second scenario.

e_{link}	P_{17}	P_{18}	P_{19}	P_{20}	P_{21}	$\bar{e}$ (m)	(%)
e_1 (m)	9.57	10.74	10.96	13.59	15.66	12.11	5.70
e_2 (m)	19.03	18.04	12.96	22.91	29.85	20.56	9.69
e_3 (m)	12.69	14.18	11.73	22.91	22.19	16.74	7.89

5.2.2 Simulation analysis. We complement the measurement-based evaluation of the system with a simulation-based analysis. The main objective is to predict the uncertainty resulting from the path loss model characterization of each link between the target and the anchor nodes, and the RSSI values of such links. In order to be more reliable, we use the standard deviation of the RSSI variable obtained from the measurement-based characterization procedure (Figure 8). We also utilize probabilistic distributions to establish a simulation set that allows to predict the behavior of the system for different locations of the target node. For the previously described 90 m × 90 m and 150 m × 150 m scenarios, Figure 9 shows the comparison of the position estimation error for the simulation results versus the evaluation based on real measurements. We observe an agreement between the simulation and the real measurements which validates our field test results.

We made additional field test evaluations including asymmetric scenarios and other rural zones around Cuenca city and the results are similar to the presented in this section.

6 CONCLUSIONS AND FUTURE WORK

In this work, firstly, we have evaluated the Semtech LoRa devices regarding their time measurement capabilities, and the quality of their RF components. This evaluation focuses on the development of a low cost LoRa-based positioning system. Although with these devices we dispose of three options for the time measurement, the field test evaluation shows that no one of the RTT estimation methods are suitable for the development of a time-based positioning system such as ToA or TDoA. On the other hand, the evaluation of the quality of the RF components focuses on the RSSI sensitivity and dynamic range. We include the analysis of two versions of Semtech devices, i.e. LoPy 1.0 and FiPy. We observe that, although both kind of devices are based on the same SX1272 chip, they exhibit different RSSI behaviors. We also determine that the useful dynamic range for a RSSI-based positioning system is values of

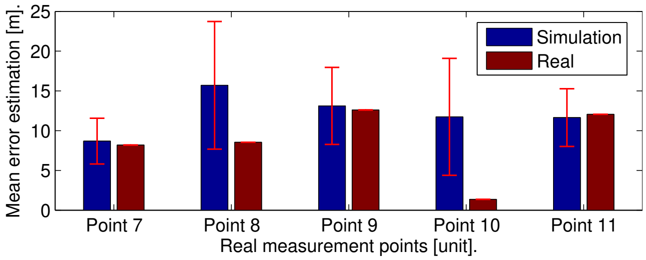

(a) 90 m×90 m scenario.

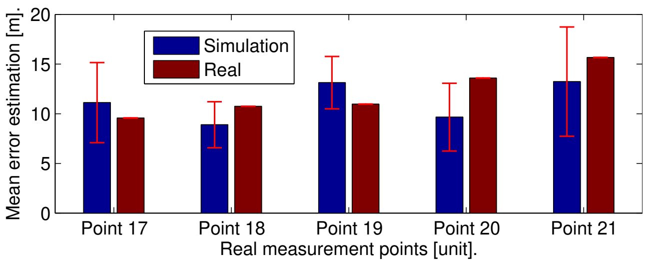

(b) 150 m×150 m scenario.

Figure 9: Simulation errors versus real measurement errors.

$RSSI > -110$ dBm. Since we are using a LPWAN technology, we really expect a wider dynamic range which would allow the positioning system to work in more extensive areas. Additionally, a deeper analysis of the real transmission power of the devices shows that LoPy 1.0 power amplifier and accessories present better quality than the FiPy one.

On this basis, we develop a RSSI-based positioning system with the trilateration algorithm and we evaluate it by means of extensive field test on different rural scenarios and environment considerations. For this low cost system, we found on average a position estimation error of around 8.55 m corresponding to a error of 6.72% for the 90 m × 90 m square scenario. Meanwhile, for the 150 m × 150 m scenario the average error is around 12.11 m corresponding to a 5.70%.

Future research will include the evaluation and use of external RTC modules in order to be able to implement a time-based positioning system. We should also consider the use of different LoRa hardware implementations which present, at similar costs, better RSSI sensitivity and dynamic range. Temperature and humidity sensors should be included in the system, in order to determine the impact of the weather conditions over the RSSI values and its variability. Although our first objective is the evaluation of LoRa for outdoor positioning systems, we will include also the evaluation for indoor environments. Finally, we will evaluate alternative methods for solving the system of equations of the trilatearion algorithm such as minimum squares or Taylor series.

REFERENCES

[1] Riaz Uddin Mondal. Radio frequency fingerprinting for outdoor user equipment localization. *Jyväskylä studies in computing*, (271), 2017. URL https://jyx.jyu.fi/handle/123456789/56222.

[2] Andreas Savvides, Chih-Chieh Han, and Mani B. Strivastava. Dynamic fine-grained localization in Ad-Hoc networks of sensors. In *Proceedings of the 7th annual international conference on Mobile computing and networking - MobiCom '01*, pages 166–179, Rome, Italy, 2001. ACM Press. ISBN 978-1-58113-422-3. doi: 10.1145/381677.381693. URL http://portal.acm.org/citation.cfm?doid=381677.381693.

[3] S. Benaissa, D. Plets, E. Tanghe, J. Trogh, L. Martens, L. Vandaele, L. Verloock, F.A.M. Tuyttens, B. Sonck, and W. Joseph. Internet of animals: characterisation of LoRa sub-GHz off-body wireless channel in dairy barns. *Electronics Letters*, 53(18): 1281–1283, August 2017. ISSN 0013-5194, 1350-911X. doi: 10.1049/el.2017.1344. URL http://digital-library.theiet.org/content/journals/10.1049/el.2017.1344.

[4] Ahmad Muzaffar Baharudin and Wanglin Yan. Long-range wireless sensor networks for geo-location tracking: Design and evaluation. In *2016 International Electronics Symposium (IES)*, pages 76–80, Denpasar, Indonesia, September 2016. IEEE. ISBN 978-1-5090-1640-2. doi: 10.1109/ELECSYM.2016.7860979. URL http://ieeexplore.ieee.org/document/7860979/.

[5] Thuraiappah Sathyan, Richard Shuttleworth, Mark Hedley, and Keith Davids. Validity and reliability of a radio positioning system for tracking athletes in indoor and outdoor team sports. *Behavior Research Methods*, 44(4):1108–1114, December 2012. ISSN 1554-3528. doi: 10.3758/s13428-012-0192-2. URL http://www.springerlink.com/index/10.3758/s13428-012-0192-2.

[6] Dhaval Patel and Myounggyu Won. Experimental Study on Low Power Wide Area Networks (LPWAN) for Mobile Internet of Things. In *2017 IEEE 85th Vehicular Technology Conference (VTC Spring)*, pages 1–5, Sydney, NSW, June 2017. IEEE. ISBN 978-1-5090-5932-4. doi: 10.1109/VTCSpring.2017.8108501. URL http://ieeexplore.ieee.org/document/8108501/.

[7] James Jin Kang, Iryna Khodasevych, and Sasan Adibi. A disaster recovery system for location identification-based low power wide area networks (LPWAN). In *2017 27th International Telecommunication Networks and Applications Conference (ITNAC)*, pages 1–6, Melbourne, VIC, November 2017. IEEE. ISBN 978-1-5090-6796-1. doi: 10.1109/ATNAC.2017.8215359. URL http://ieeexplore.ieee.org/document/8215359/.

[8] Sujuan Liu, Chuyu Xia, and Zhenzhen Zhao. A low-power real-time air quality monitoring system using LPWAN based on LoRa. In *2016 13th IEEE International Conference on Solid-State and Integrated Circuit Technology (ICSICT)*, pages 379–381, Hangzhou, China, October 2016. IEEE. ISBN 978-1-4673-9717-9 978-1-4673-9719-3. doi: 10.1109/ICSICT.2016.7998927. URL http://ieeexplore.ieee.org/document/7998927/.

[9] Sigfox. Sigfox. URL https://www.sigfox.com/.

[10] Nikolay S. Knyazev, Victor A. Chechetkin, and Denis A. Letavin. Comparative analysis of standards for Low-power Wide-area Network. In *2017 Systems of Signal Synchronization, Generating and Processing in Telecommunications (SINKHROINFO)*, pages 1–4, Kazan, Russia, July 2017. IEEE. ISBN 978-1-5386-1786-1. doi: 10.1109/SINKHROINFO.2017.7997528. URL http://ieeexplore.ieee.org/document/7997528/.

[11] Orestis Georgiou and Usman Raza. Low Power Wide Area Network Analysis: Can LoRa Scale? *IEEE Wireless Communications Letters*, 6(2):162–165, April 2017. ISSN 2162-2337, 2162-2345. doi: 10.1109/LWC.2016.2647247. URL http://ieeexplore.ieee.org/document/7803607/.

[12] Bogdan Oniga, Vasile Dadarlat, Eli De Poorter, and Adrian Munteanu. Analysis, design and implementation of secure LoRaWAN sensor networks. In *2017 13th IEEE International Conference on Intelligent Computer Communication and Processing (ICCP)*, pages 421–428, Cluj-Napoca, September 2017. IEEE. ISBN 978-1-5386-3368-7. doi: 10.1109/ICCP.2017.8117042. URL http://ieeexplore.ieee.org/document/8117042/.

[13] Pierre Neumann, Julien Montavont, and Thomas Noel. Indoor deployment of low-power wide area networks (LPWAN): A LoRaWAN case study. In *2016 IEEE 12th International Conference on Wireless and Mobile Computing, Networking and Communications (WiMob)*, pages 1–8, New York, NY, October 2016. IEEE. ISBN 978-1-5090-0724-0. doi: 10.1109/WiMOB.2016.7763213. URL http://ieeexplore.ieee.org/document/7763213/.

[14] Seyed A. Reza Zekavat and R. Michael Buehrer, editors. *Handbook of Position Location: Theory, Practice, and Advances.* John Wiley & Sons, Inc., Hoboken, NJ, USA, September 2011. ISBN 978-1-118-10475-0 978-0-470-94342-7. doi: 10.1002/9781118104750. URL http://doi.wiley.com/10.1002/9781118104750.

[15] Tim Hadwen, Vanessa Smallbon, Qing Zhang, and Matthew D'Souza. Energy efficient LoRa GPS tracker for dementia patients. In *2017 39th Annual International Conference of the IEEE Engineering in Medicine and Biology Society (EMBC)*, pages 771–774, Seogwipo, July 2017. IEEE. ISBN 978-1-5090-2809-2. doi: 10.1109/EMBC.2017.8036938. URL https://ieeexplore.ieee.org/document/8036938/.

[16] Bernat Carbones Fargas and Martin Nordal Petersen. GPS-free geolocation using LoRa in low-power WANs. In *2017 Global Internet of Things Summit (GIoTS)*, pages 1–6, Geneva, Switzerland, June 2017. IEEE. ISBN 978-1-5090-5873-0. doi: 10.1109/GIOTS.2017.8016251. URL http://ieeexplore.ieee.org/document/8016251/.

[17] Lora alliance. URL https://lora-alliance.org/.

[18] Pycom. Pycom. URL https://pycom.io/.

[19] Pycom. Datasheet fipy. Datasheet, Pycom, 2018. URL https://docs.pycom.io/.gitbook/assets/fipy-specsheet-1.pdf. Versión 1.0.

[20] Pycom. Datasheet lopy versión 1.0. Datasheet, Pycom, 2018. URL https://docs.pycom.io/.gitbook/assets/lopy-specsheet.pdf. Versión 1.0.

[21] Semtech. Semtech. URL https://www.semtech.com/.